Research Article

Use of Cu(II)-incorporated zeolite Y for decolourization of dyes in water: a case study with aqueous methylene blue and Congo red

Smita Chowdhury[1] · **Krishna G. Bhattacharyya**[1]

Abstract
Removal of colour from wastewater discharged by textile and dying industries is a major environmental issue. Catalytic wet air oxidation (CWAO) has emerged as one of the most acceptable, easy and environmental friendly techniques for the treatment of organic pollutants present in wastewater. The present work explores the decolourization of methylene blue and Congo red from aqueous solution by CWAO process using Cu(II)-incorporated zeolite Y as catalyst. The catalyst was prepared by refluxing zeolite Y with aqueous 1 M $Cu(NO_3)_2{\cdot}3H_2O$ for 6 h. The prepared catalyst was characterized by XRD, FTIR, atomic absorption spectroscopy, SEM, EDAX, BET surface area and pore volume measurement. The oxidation was carried out in a stirred reactor with pH, temperature, amount of catalyst, dye concentration and interaction time as the process variables. Both the oxidation processes follow second-order kinetics. Almost 70% conversion of methylene blue and 90% conversion of Congo red could be achieved under optimum conditions. The results indicate that Cu(II)-incorporated zeolite Y is a promising catalyst for the removal of both cationic and anionic dyes.

Keywords CWAO · Methylene blue · Congo red · Zeolite Y

1 Introduction

A dye is defined as a coloured substance that has an affinity to the substrate to which it is being applied and gives a permanent colour to them. One of the main sources of water pollution is the textile industries and their wastewater containing dyes. It is observed that more than 10–25% of the dyes are lost during dyeing process and 2–20% are released into the environment as wastewater [1]. The direct discharge of wastewater results in high amount of colour, turbidity, pH, temperature, chemical oxygen demand (COD), biochemical oxygen demand (BOD), etc., in natural water bodies which not only pollutes the water but also affects flora and fauna [2, 3]. For these adverse effects, it is necessary to remove coloured constituents of these dyes for the well-being of human and more importantly to protect our environment.

Among various dyes used in industries, methylene blue [3,7-bis(dimethylamino)-phenothiazine-5-ium chloride] is a cationic thiazine dye that is used mainly in cotton, fibres and leather [4]. The dye was previously used as a medicine, but due to its toxicity its use is no longer recommended. The main toxicity of methylene blue includes headache, vomiting, fever, confusion, high blood pressure and much other allergic reaction [5]. Congo red [1-naphthalene sulphonic acid, 3,3′-(4,4′-biphenylenebis(azo)bis(4-amino-) disodium salt] is an anionic diazo dye and is widely used in textile, rubber, paper and plastic industries [6]. The dye is known to possess carcinogenicity and may lead to tumour formation among humans. It also causes irritation of eyes and skin, vomiting and diarrhoea. Thus, use of Congo red has been banned in many countries [7]. In the present context, both methylene blue and Congo red are taken as model dyes for wastewater treatment.

Due to the complex aromatic structures, dyes are stable to heat, light and oxidizing agents and are difficult to biodegrade. Different physico-chemical methods such as advanced oxidation processes (AOP) [8], adsorption

✉ Smita Chowdhury, smitachowdhury5@gmail.com | [1]Department of Chemistry, Gauhati University, Guwahati, Assam 781014, India.

SN Applied Sciences (2019) 1:87 | https://doi.org/10.1007/s42452-018-0094-8

Received: 1 September 2018 / Accepted: 29 November 2018 / Published online: 10 December 2018

[9], electro-coagulation [10], membrane filtration [11] and coagulation [12] are used for degradation of dyes in water. Among these, adsorption techniques have received much attention for removing pollutants from wastewater using efficient adsorbents such as activated carbon, nanoparticles, polymers, carbon nanotubes and other low-cost adsorbents [13–18]. These processes, in spite of having higher efficiency for removal of dyes in wastewater, have been limited by high sludge production, high cost and regeneration or disposal of secondary pollutant [19].

Recently, many researchers have pointed out that advanced oxidation processes (AOP) can be regarded as potential alternative for wastewater treatment as they produce no hazardous sludge and generation of hydroxyl radicals during these processes can non-selectively oxidize majority of organic pollutant present in water [20, 21]. There are mainly three types of AOPs based on the type of oxidant, viz. oxygen, ozone and hydrogen peroxide. Among these AOPs, wet air oxidation (WAO) with the generation of active oxygen species like hydroxyl radicals has found to be a promising method for decolouration of dyes and for destruction of hazardous materials. However, requirement of high pressure (0.5–20 MPa) and high temperature (175–320 °C) limits the application of this process [22]. On the other hand, catalytic wet air oxidation (CWAO) requires low energy and can be carried out under mild conditions. Therefore, it has attracted considerable interest for the degradation of dyes in water [23, 24]. Various solid catalysts such as mixed metal oxides [25, 26], carbon material [27, 28], zeolites [29, 30] and clays [31, 32] have been used as supporting materials for CWAO. In particular, zeolites modified with various transition metal ions such as Fe, Cu, Co, Ni, Mn have been found to be promising catalysts for the oxidation of various organic pollutants [33]. Tekbas et al. [34] studied the decolourization of an azo dye (Reactive Orange 16) by using Fe-exchanged zeolite. They reported that more than 90% decolourization of the dye was achieved in 60 min at pH 5.7, temperature 35 °C and catalyst load 1.0 g L^{-1} in the presence of 15 mml H_2O_2. Similar type of results was obtained by Kondro et al. [30] for the degradation of another azo dye (Congo red) using Fe-exchanged zeolite Y as a catalyst.

In the present work, Cu(II)-incorporated zeolite Y was used as catalyst for the oxidation of one cationic dye (methylene blue) and one anionic dye (Congo red) in aqueous medium. The oxidation was carried out at atmospheric pressure with process variables such as pH, temperature, amount of catalyst, dye concentration and interaction time to evaluate the optimum conditions. The importance of the work lies in the fact that very simple wet impregnation method was adopted for the incorporation of metal ion into zeolite surface and the oxidation process did not need an external oxidizing agent, thereby making the process cost-effective.

2 Materials and methods

2.1 Materials

The chemicals used in this work were zeolite Y (Himedia Laboratory Private, India), $Cu(NO_3)_2{\cdot}3H_2O$ (Merck Mumbai), methylene blue (Merck Mumbai), Congo red (Merck Mumbai), H_2SO_4 (Merck Mumbai) and NaOH (Merck Mumbai). All reagents were used without further purification.

2.2 Preparation of catalyst

The incorporation of Cu(II) ion into zeolite surface was done by wet impregnation method in which the solid support was mixed with a small volume of aqueous metal salt solution. For this, the commercially available Na-Y zeolite was washed with double-distilled water and dried. Then, 25 g of zeolite Y was refluxed with 100 mL of 1.0 M $Cu(NO_3)_2{\cdot}3H_2O$ solution for 6 h in a 500-mL round-bottom flask. The mixture was separated by filtration and washed with distilled water for several times. It was then dried in an oven, calcined at 500 °C for 5 h in a muffle furnace and preserved in stoppered glass bottle.

2.3 Preparation of dye solutions

A stock solution of the dyes, methylene blue and Congo red, containing 1000 mg L^{-1} was prepared in double-distilled water. The aqueous solution of methylene blue had a pH of 7.5 and that of Congo red had 6.5. The structures of methylene blue (basic dye) and Congo red (acid dye) are shown in Fig. 1.

2.4 Characterizations

The surface functional groups of the catalyst were measured by FTIR measurements (Perkin Elmer Spectrum RXI, range 4000–450 cm^{-1}) using KBr self-supported pellet technique. The crystalline structure of the material was done with X-ray diffraction (XRD) measurements (Philips Analytical X-Ray Spectrophotometer, PW 1710, Cu Ka radiation). The amount of Cu(II) entering the zeolite Y was determined with atomic absorption spectrophotometer (AAS; Perkin Elmer AAnalyst 220). The surface topography and elemental composition of the prepared catalysed was observed with scanning electron microscopy (SEM) measurements (JEOL JSW-6360) coupled with an energy-dispersive X-ray spectrometer (EDX). Brunauer–Emmett–Teller (BET) surface area and the pore volume of the catalyst

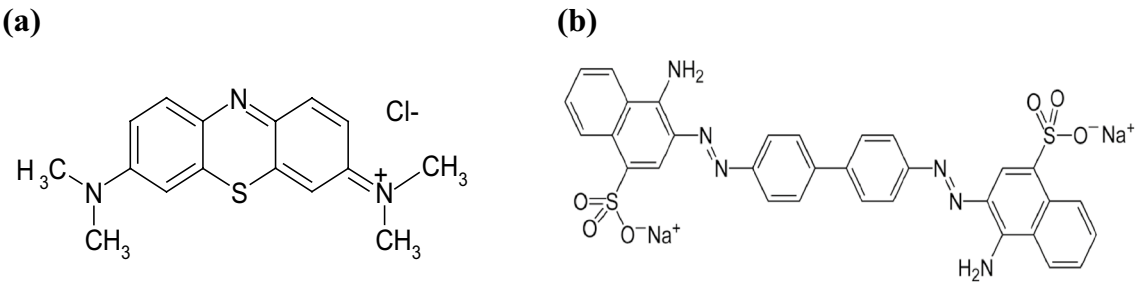

Fig. 1 Structure of the dyes, **a** methylene blue; **b** Congo red

were measured with nitrogen sorption apparatus (Micromeritics Tristar surface area and porosity analyser). The pore size distribution was determined by using Barrett–Joyner–Halenda (BJH) method.

2.5 Catalytic oxidation

The oxidation was carried out in a water bath shaker (NSW, New Delhi, India) in 50-mL Erlenmeyer flasks. Twenty millilitres of each dye solution was mixed with a pre-weighted amount of the catalyst and agitated for a fixed interval of time. The mixture was centrifuged (Remi Research Centrifuge, R24) for 15 min at a speed of 6000 rpm, and the unconverted reactant in supernatant liquid was determined spectrophotometrically (Shimadzu 1800 UV–Visible Spectrometer).

For evaluation of catalytic activity, the percentage conversion of dye is calculated using the expression:

$$\%\ \text{conversion} = \left[(C_i - C_f)/C_i\right] \times 100\%, \quad (1)$$

where C_i and C_f are the initial and final concentration (mg L^{-1}) of the dye, respectively.

2.6 Monitoring chemical oxygen demand

Chemical oxygen demand (COD) reduction in the reaction mixture was determined by open reflux method [35]. In this method, 10 mL of the dye solution was mixed with 20 mL 0.0417 M $K_2Cr_2O_7$ solution, 30 mL conc. H_2SO_4 and a pinch of silver sulphate along with glass beads. The reaction mixture was refluxed for 2 h and then cooled. Then, 80 mL distilled water was added to the mixture and was titrated with 0.25 M ferrous ammonium sulphate (FAS) solution using ferroin indicator to determine the amount of unreacted $Cr_2O_7^{2-}$. The whole procedure is first done with a blank (10 mL of distilled water in place of dye solution). COD was calculated from the following formula:

$$\text{COD (mg L}^{-1}) = [(B - S) \times M \times 8000]/V, \quad (2)$$

where B is the volume of FAS used for blank titration; S, volume of FAS used for titration of dye solution; M, molarity of FAS; V, volume of the dye solution taken. The percentage COD removal is calculated by the formula:

$$\%\text{COD removal} = \left[(\text{COD}_0 - \text{COD}_t)/\text{COD}_0\right] \times 100\%, \quad (3)$$

where COD_0 and COD_t are the COD of the reaction mixture at $t = 0$ and $t = t$, respectively.

3 Results and discussion

3.1 Characterizations of zeolite Y and Cu(II)–zeolite Y

The FTIR spectra for zeolite Y and Cu(II)–zeolite Y are depicted in Fig. 2. The observed frequencies of zeolite Y at 460, 570, 708, 1004, 1432, 1635 and 3432 cm^{-1} are in good agreement with the data of the previous literature [33]. Incorporation of Cu(II) into the zeolite surface leads to the changes in the characteristic bands around 500–1300 cm^{-1}. The band around 400–550 cm^{-1} corresponds to Si–O–Si bending and that around 660–860 cm^{-1} corresponds to stretching of $(SiAl)O_4$ building block [36]. Shift of these bands with considerable change in intensity signifies the incorporation

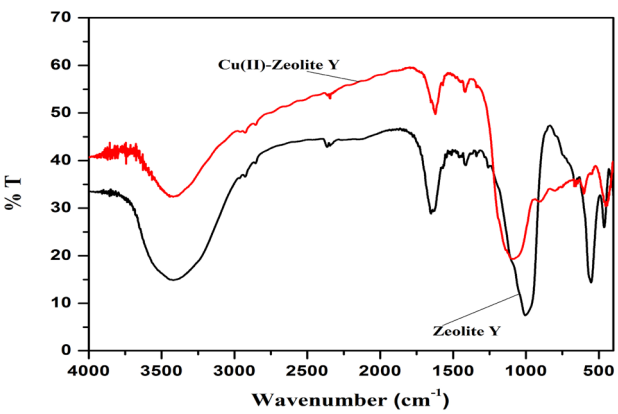

Fig. 2 FTIR of zeolite Y and Cu(II)–zeolite Y

of Cu(II) with the external linkage of tetrahedral units. In addition, the product obtained after impregnation shows pale blue colour that is the primary evidence of the incorporation of Cu(II) ion into zeolite surface.

The XRD patterns of zeolite Y and Cu(II)–zeolite Y in the 2θ values ranging from 5° to 80° are shown in Fig. 3. As shown in Fig. 3a, the characteristic peaks of zeolite Y at 2θ values of 6.3, 10.3, 12.1, 15.9, 20.7, 24.0, 27.5 and 31.95 correspond to (111), (220), (311), (331), (440), (533), (642) and (555), respectively, which agree well with the previous studies of Hriljac et al. [37]. XRD patterns show that after the incorporation of Cu(II) into zeolite, the crystalline structure of zeolite Y changed significantly (Fig. 3b). Here, the complete diminishing of zeolite peaks indicates the high metal loading on zeolite surface. Similar results are obtained by Kondro et al. [30], showing that high loading of transition metal considerably affected the crystallinity of the support. In addition, the XRD pattern of the Cu(II)–zeolite Y show two high-intensity peaks at 2θ values of 35.5 and 38.7 which could be indexed to (11-1) and (111) reflections of monoclinic CuO crystallite (PDF files 48–1548). The presence of the high-intensity peaks proved the presence of considerable Cu(II) particles inside the pore of zeolite [36].

We had carried out AAS measurement to determine the amount of Cu(II) entering the zeolite Y. For this purpose, a pre-weighted catalyst was digested with tri-acid mixture (conc. HNO_3/HCl/H_2SO_4 = 1:2:4). It was found that the amount of Cu in zeolite Y was 17.06 mg/kg which was quite high enough compared to the amount of Cu already present in zeolite Y (0.037 mg/kg). Thus, we can say that Cu(II) had very high affinity for zeolite Y.

Scanning electron micrographs of zeolite Y and Cu(II)–zeolite Y are presented in Fig. 4a, b. On comparing the SEM images of zeolite Y (Fig. 4a) and Cu(II)–zeolite Y (Fig. 4b), we had not observed any major change in their morphologies except a little loss of uniformity in the crystal size distribution after Cu(II) incorporation. This observation suggested that Cu(II) ion might be located inside the pores of zeolite Y. Similar results were obtained by Chen et al. [38], showing that due to the porous structure of zeolite Y, its available surface area was fully occupied by incorporated metal ions. As a result, these metal ions were invisible on the surface of zeolite Y.

The presence of Cu(II) species was further checked with EDAX. The EDAX measurement confirms the presence of almost 7 weight% of Cu over zeolite Y (inside Fig. 4c). In addition, low peaks of Cu in the EDX spectra for Cu(II)–zeolite Y support the fact that metal species was located inside the zeolite structure (Fig. 4c).

Finally, the presence of Cu ion was confirmed by nitrogen sorption isotherm and the results are shown in Fig. 4d. The reduction in the volume of nitrogen adsorbed at the low value of P/P_o indicates unavailability of microporosity after incorporation. The Cu(II)-incorporated zeolite Y produced a large decrease in BET surface area of zeolite Y from 485 to 287 $m^2\ g^{-1}$. In the meantime, the pore volume of zeolite Y and Cu(II)–zeolite Y was 0.35 and 0.12 $cm^3\ g^{-1}$, respectively. This large decrease in surface area as well as pore volume after incorporation is consistent with the loss of crystallinity of zeolite [33]. Rache et al. [39] found similar large decrease in surface area from 432 to 259 $m^2\ g^{-1}$ and pore volume from 0.24 to 0.10 $cm^3\ g^{-1}$ of zeolite Y while exchanging with Fe ion for the degradation of Orange II dye. Aravindhan et al. [40] reported that

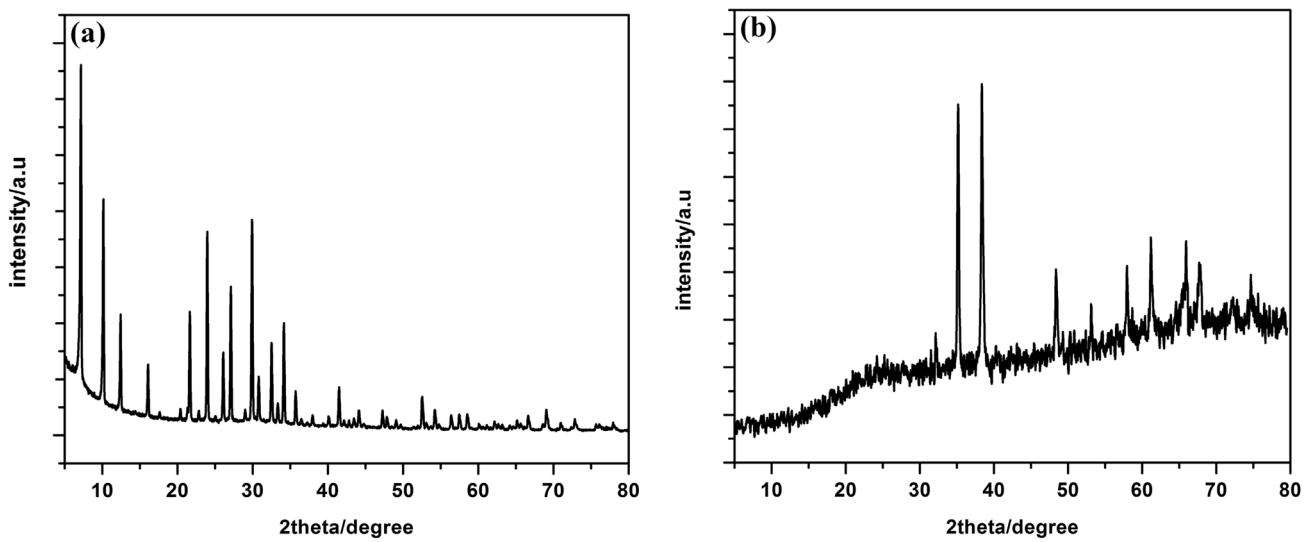

Fig. 3 X-ray powder diffraction patterns of zeolite Y (**a**) and Cu(II)–zeolite Y (**b**)

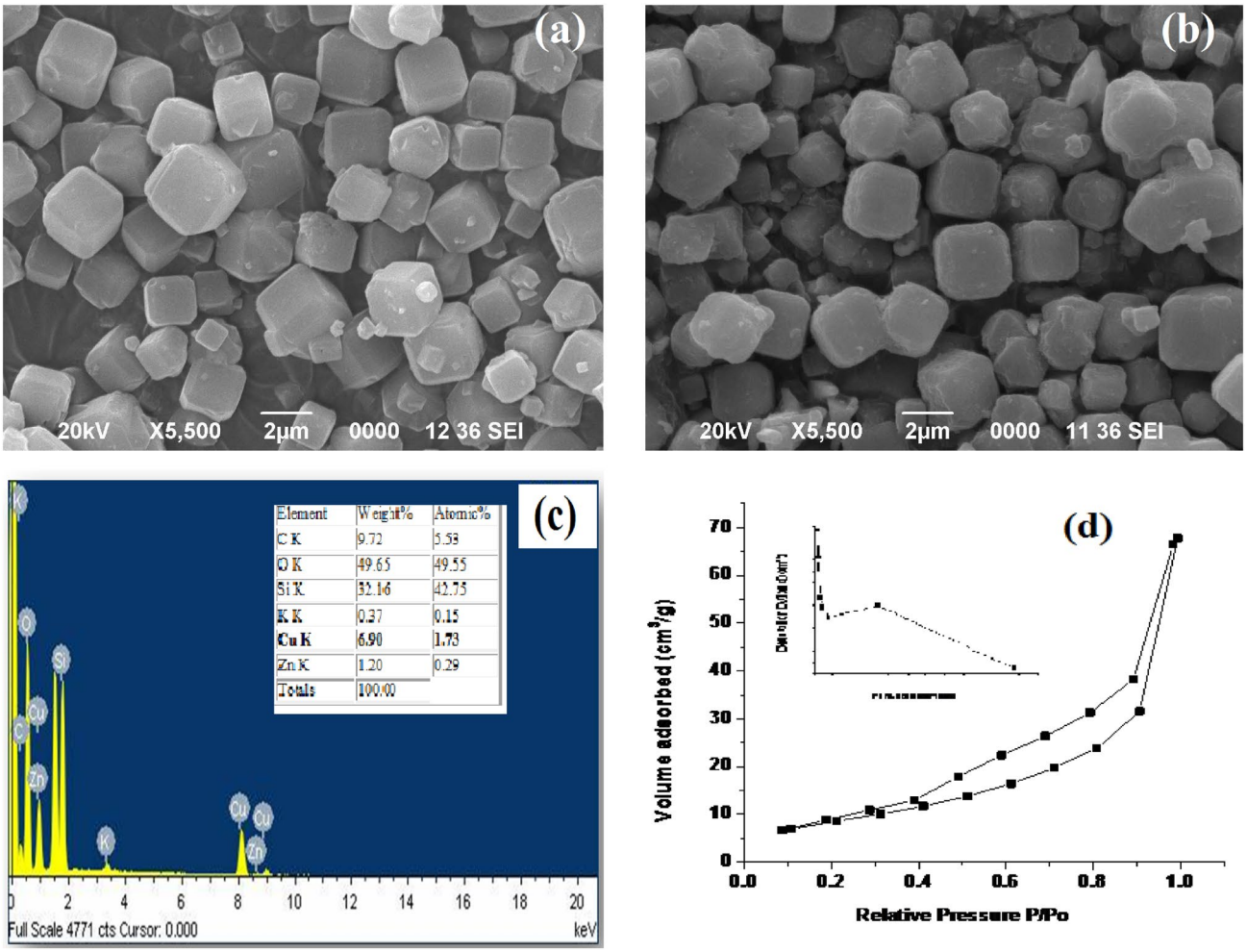

Fig. 4 SEM image of zeolite Y (**a**) and Cu(II)–zeolite Y (**b**); energy-dispersive X-ray analysis pattern of Cu(II)–zeolite Y (**c**) and nitrogen sorption isotherm of Cu(II)–zeolite Y (the inset shows its pore size distribution) (**d**)

decrease in surface area of doped zeolite Y was due to the incorporation of high concentration of metal ion inside the zeolite surface. However, a different result was obtained by Kondru et al. [30] as the BET surface area of zeolite Y slightly decreased from 433 to 423 $m^2\ g^{-1}$ after doping with Fe ion. They recommended that small decrease in surface area after doping was due to the low loading of metal ion and its insertion did not produce any significant affect to the support. Based on the above facts, it can be concluded that, in the present work, high concentration of Cu ion was successfully incorporated inside zeolite Y.

3.2 Wet oxidation of methylene blue and Congo red

3.2.1 Kinetics of dye degradation

The degradation of methylene blue and Congo red was carried out with both raw and modified zeolite Y using catalyst load of 1.5 g L^{-1} and dye concentration 10.0 mg L^{-1} at room temperature and atmospheric pressure. It was found that for methylene blue the percentage degradation was 22.08–52.65% (zeolite Y) and 41.89–67.87% (Cu(II)-incorporated zeolite Y) when the reaction time was increased from 5 to 300 min (Fig. 5a). For the same time period, Congo red degradation percentage was 7.44–26.38% for zeolite Y and 47.22–87.63% for Cu(II)-incorporated zeolite Y (Fig. 5b). In all cases, the degradation process achieved equilibrium condition at about 240 min. Interestingly, with Cu(II)-incorporated zeolite Y more than 40% conversion of dyes (for both methylene blue and Congo red) was achieved within 5 min. At the same time, no measurable conversion of methylene blue or Congo red dye was obtained in the absence of catalyst after 5-h reaction.

These catalytic reactions were tested for second-order kinetics using the following equation:

$$dC/dt = k(C_0 - C_t)^2 \quad (4)$$

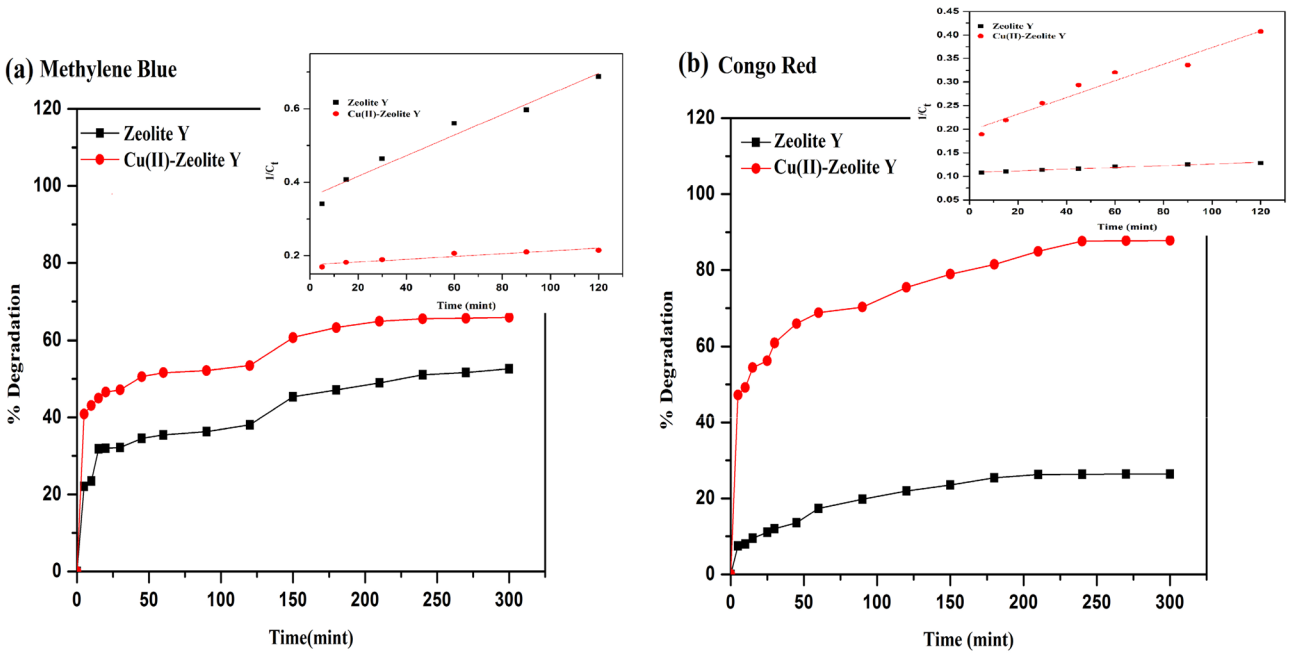

Fig. 5 Catalytic degradation of methylene blue (**a**) and Congo red (**b**) by zeolite Y and Cu(II)–zeolite Y. Inset: plots of second-order kinetics for methylene blue (**a**) and Congo red (**b**). Concentration of the dye solution 10 mg L^{-1}; mass of catalyst 1.5 gL. $^{-1}$

or $1/C_t = kt + 1/C_0$, (5)

where C_0 and C_t are initial concentration and concentration at any time (t), respectively, and k is the second-order rate constant. The plot of $1/C_t$ versus time was straight lines (inset of Fig. 5a, b) in all cases with regression coefficient $R = 0.95 - 0.97$. Singh et al. [36] have shown that degradation of Congo red with Cu-impregnated zeolite Y followed first-order kinetics. In the present work, first-order kinetics were also tested but deviated much from linearity.

3.2.2 Effects of catalyst loading

The effects of catalyst loading on dye degradation were investigated at different catalyst concentrations (0.5–2.0 g L^{-1}) to obtain an optimum catalyst loading for maximum conversion.

As depicted in Fig. 6a, b, oxidation of both the dyes increases with increase in catalyst loading from 0.5 to 1.5 g L^{-1} (dye concentration 10.0 mg L^{-1}, temperature 303 K, reaction time 4 h).This can be attributed to the presence of sufficiently large number active sites on the surface of zeolite Y. However, on further increase in catalyst load to 2 g L^{-1} the degradation remained almost unchanged. This may be due to the reason that increased catalyst load leads to aggregation of solid particles, thereby reducing the surface area as well as active sites. As a result, no further increase in oxidation was observed. Similar results were obtained by Singh et al. [36] for the degradation of Congo red with Cu-impregnated zeolite Y as catalyst. Thus, the catalyst load of 1.5 g L^{-1} was taken as optimum value in the present case. In addition, with raw zeolite Y Congo red degradation was only 25.57% (Fig. 6b) which was increased more than three times with Cu(II)-incorporated zeolite Y.

3.2.3 Effects of dye concentration

The effects of dye concentration on oxidative conversion of methylene blue and Congo red were studied in five concentrations of 1.0, 5.0, 10.0, 50.0 and 100.0 mg L^{-1} by keeping other parameters constant. It was found that degradation percentage increased with increase in concentration of dye up to 10.0 mg L^{-1} and then it decreased significantly (Fig. 7a). Tayade et al. [41] observed similar type of methylene blue degradation using ultraviolet light-emitting diodes. They suggested that increased dye concentration required large catalyst surface for the conversion and as the catalyst surface remained the same the degradation had to decrease. Thus, in the present case, the optimal dye concentration of methylene blue or Congo red was 10.0 mg L^{-1}.

3.2.4 Effects of pH

To study the effect of pH on dye degradation, the pH of the dye solution was adjusted by adding dropwise 0.1 N HNO_3 or 0.1 N NaOH solution. Methylene blue dimerizes and

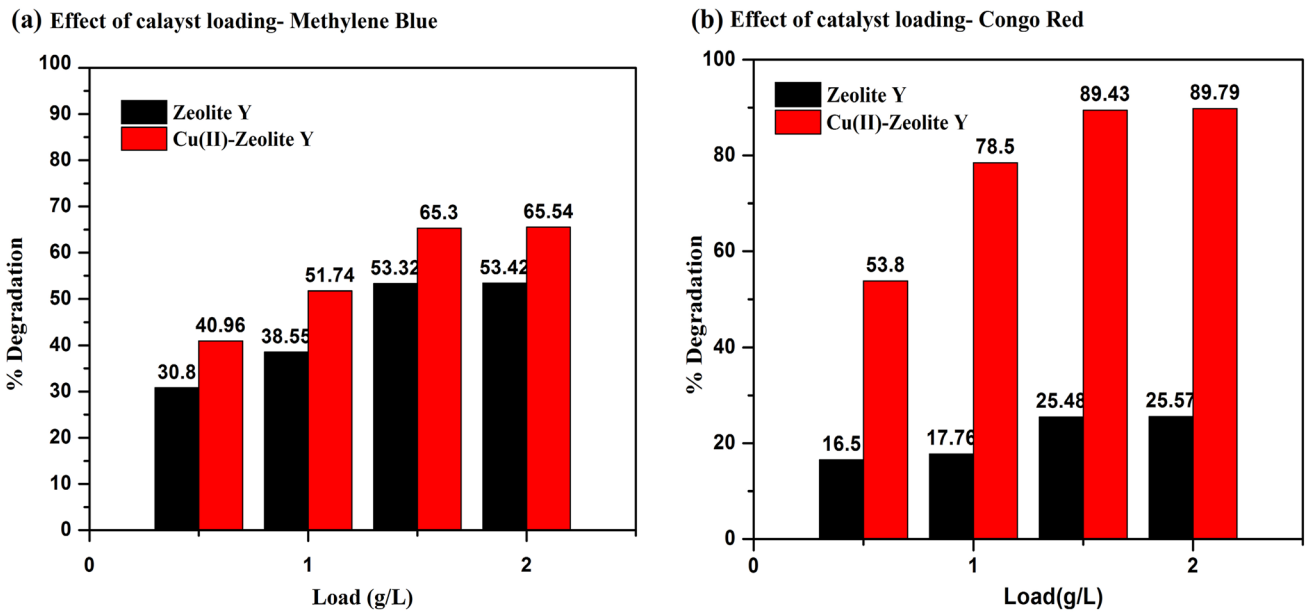

Fig. 6 Effects of catalyst loading: methylene blue (**a**) and Congo red (**b**) using zeolite Y and Cu(II)–zeolite Y

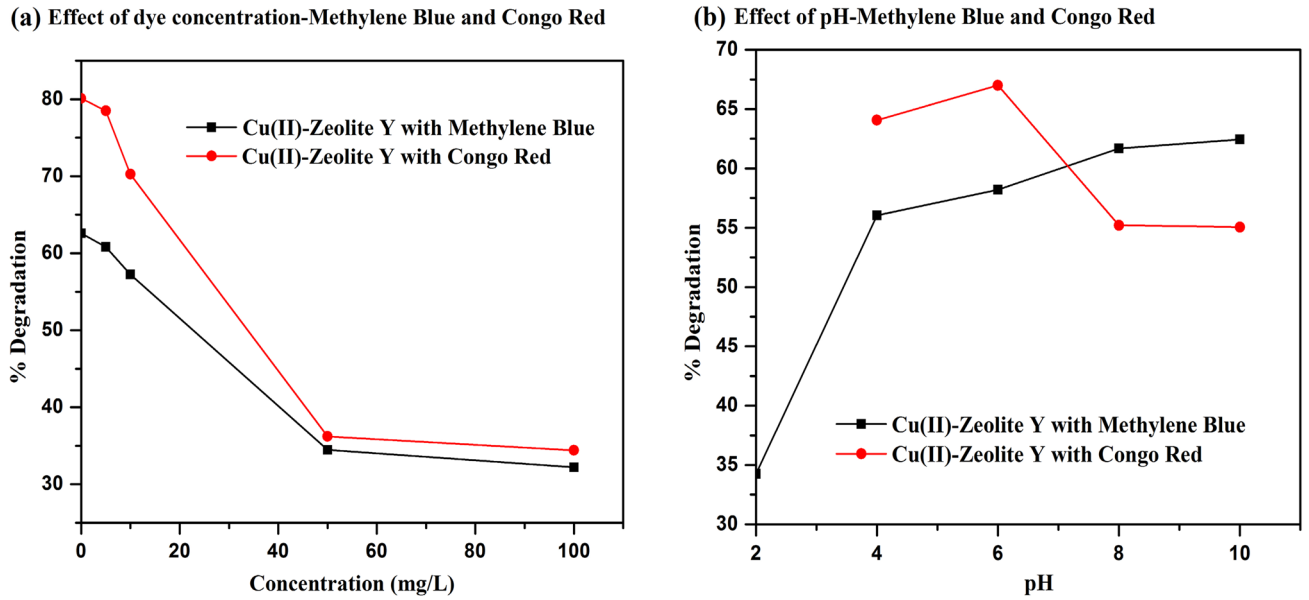

Fig. 7 Effect of dye concentration (**a**) and pH (**b**) on methylene blue and Congo red using Cu(II)–zeolite Y

changes its colour at pH = 11.0 and above. Being a cationic dye, methylene blue degradation increases with increase in pH value. Thus, in the present case its degradation was minimum at pH 2.0 and maximum at pH 10.0 (Fig. 7b) with a catalyst load of 1.5 g L^{-1} and dye concentration 10.0 mg L^{-1}. On the other hand, Congo red, an anionic dye, is very sensitive dye to pH. It develops blue colour at pH < 5 and deep red colour at pH > 10 [42]. Thus, the effects of pH on Congo red degradation were studied in the pH range 6.0–10.0 using 1.5 g L^{-1} of catalyst and 10.0 mg L^{-1} of dye solution. As shown in Fig. 7b, with Cu(II)-incorporated zeolite Y, the degradation percentage of Congo red increased with increase in pH until it reaches a maximum value at pH 6 and thereafter it decreased and became almost constant. The final pH of the treated solutions was also measured using a pH meter. A regular decrease in final pH value to near-neutral pH was observed. This decrement in pH can be associated with the formation of carbon dioxide,

mineral acids and other harmless intermediate products [36]. In addition to the determination of the concentration of leached Cu(II) ion, the solution was analysed at different pH values (2.0, 4.0, 6.0, 8.0 and 10.0) by AAS measurement. It was observed that Cu(II) concentration decreased from 16.85 to 2.61 mg L^{-1} with an increase in pH value. Thus, in acidic medium the leaching of Cu(II) ion was highly significant. Hence, all the experiments were carried out at the natural pH of the respective dye solution.

3.2.5 Effects of temperature

With increase in temperature from 20 to 50 °C, the percentage degradation of methylene blue increased from 62.36 to 79.70% and that of Congo red increased from 67.22 to 94.05%, respectively. Nezamzadeh-Ejhieh and Shahriari [33] reported that higher temperature reduced the solubility of oxygen in water and produced significant evaporation of the reacting solution. Thus, the temperature more than 40 °C was not recommended by them. Therefore, in our present case normal room temperature (30 °C) was taken as experimental temperature, although the performance of degradation processes was not as fast as at higher temperature.

3.2.6 COD measurement

It was observed that the initial COD load of methylene blue (10.0 mg L^{-1}, catalyst load 1.0 g L^{-1}, reaction time 5–300 min at room temperature and atmospheric pressure) decreased from 1420 to 220 mg L^{-1} (overall COD reduction 84.5%). The COD reduction in Congo red under identical condition decreased from 1450 to 135 mg L^{-1} (overall COD reduction 90.7%). The large reduction in COD clearly indicated the oxidation of both the dyes to simple organic compounds as well as complete mineralization. Kondru et al. [30] have found 58% removal of COD for Congo red at pH 7, 90 °C using 0.6 mL H_2O_2/350 mL solution and 1.0 g L^{-1} Fe-exchanged zeolite Y as catalyst. On the other hand, Dutta et al. [43] observed 89% removal of COD for methylene blue using Fe^{2+}–H_2O_2 in a Fenton-type reaction at room temperature and atmospheric pressure.

3.2.7 Recovery and reuse of the catalyst

The reusability of Cu(II)-incorporated zeolite Y was tested on the basis of its catalytic activity up to three consecutive runs. It was found that for first, second and third run the maximum degradation of methylene blue was 68.52, 65.42 and 61.53% and that of Congo red was 87.72, 84.52 and 79.63%, respectively. Thus, the catalyst showed almost same activity (decreased by 4–5%) for the oxidative degradation of both the dyes.

4 Conclusion

We have incorporated here Cu(II) ion into zeolite Y via wet impregnation method. Our result showed that Cu(II)–zeolite Y could be a promising catalyst for the oxidative degradation of both cationic dye (methylene blue) and anionic dye (Congo red). The successful incorporation of Cu(II) into zeolite Y was confirmed by different characterization methods (AAS, FTIR, XRD, SEM, EDAX and BET surface area). The catalyst showed higher catalytic activity for Congo red than methylene blue by using a catalyst load of 1.5 g L^{-1} and dye concentration of 10.0 mg L^{-1} at room temperature and atmospheric pressure. Considering low leaching of Cu at near-neutral pH, the respective natural pH of the dye was taken as optimum pH. The reactions followed second-order kinetics. Again, the catalyst can be used successfully up to three consecutive runs. Thus, these materials have great potential for oxidizing hazardous dye pollutants from wastewater and its application in practical environmental cleanup needs further effort.

Acknowledgements The authors gratefully acknowledged the instrument support of SIF, Gauhati University and IASST, Guwahati. We are also thankful to both the reviewers for their suggestion to improve the quality of the manuscript.

Compliance with ethical standards

Conflict of interest The authors declare that they have no competing interests.

References

1. Emami F, Tehrani-Bagha AR, Gharanjig K, Menger FM (2010) Kinetic study of the factors controlling Fenton-promoted destruction of a non-biodegradable dye. Desalination 257:124–128
2. Hammami S, Bellakhal N, Oturan N, Oturan MA, Dachraoui M (2008) Degradation of acid orange 7 by electrochemically generated ·OH radicals in acidic medium using a boron-doped diamond or platinum anode: a mechanistic study. Chemosphere 73:678–684
3. Herney-Ramirez J, Silva AMT, Vicente MA, Costa CA, Madeira LM (2011) Degradation of avid orange 7 using a saponite-based catalyst in wet hydrogen peroxide oxidation: kinetic study with Fermi's equation. Appl Catal B Environ 101:197–205
4. Sahoo C, Gupta AK (2012) Optimization of photocatalytic degradation of methyl blue using silver ion doped titanium dioxide by combination of experimental design and response surface approach. J Hazard Mater 215:302–310
5. Miclescu A, Wiklund L (2010) Methylene blue, an old drug with new indications? Jurnalul Roman de Anestezie Terapie Intensive 17:35–41
6. Hu Z, Chena H, Ji F, Yuana S (2010) Removal of congo red from aqueous solution by cattail root. J Hazard Mater 173:292–297

7. Jalandoni-Buan AC, Decena-Soliven ALA, Cao EP, Barraquio VL, Barraquio WL, Baun ACJ (2010) Characterization and identification of congo red decolorizing bacteria from monocultures and consortia. Phillpp J Sci 1:71–78
8. Esther F, Cserhati T, Gyula O (2004) Removal of synthetic dyes from wastewaters: a review. Environ Int 30:953–971
9. Ali I, Gupta V (2007) Advances in water treatment by adsorption technology. Nat Protoc 1:2661–2667
10. Kalyani K, Balasubramaniam N, Srinivasakannan C (2009) Decolorization and COD reduction of paper industrial effluent using electro-coagulation. Chem Eng J 151:97–104
11. Dass A, Hamdaoui O (2010) Extraction of anionic dye from aqueous solution by emulsion liquid membrane. J Hazard Mater 178:973–981
12. Morshedi D, Mohammadi Z, Akbar Boojar MM, Aliakbari F (2013) Using protein nanofibrils to remove azo dyes from aqueous solution by the coagulation process. Colloids Surf B Biointerfaces 112:245–254
13. Zare K, Gupta VK, Moradi O, Makhlouf ASH, Sillanpaa M, Nadagouda MN, Sadegh H, Shahryari-ghoshekandi R, Pal A, Wang Z, Tyagi I, Kazemi M (2015) A comparative study on the basis of adsorption capacity between CNTs and activated carbon as adsorbents for removal of noxious synthetic dyes: a review. J Nanostruct Chem 5:227–236
14. Arabi SMS, Lalehloo RS, Olyai MRTB, Ali GAM, Sadegh H (2018) Removal of congo red azo dye from aqueous solution by ZnO nanoparticles loaded on multiwall carbon nanotubes. Phys E Low Dimens Syst Nanostruct 106:150–155
15. Agarwal S, Sadegh H, Monajjemi M, Hamdy AS, Ali GAM, Memar AOH, Shahryari-ghoshekandi R, Tyagi I, Gupta VK (2016) Efficient removal of toxic bromothymol blue and methylene blue from wastewater by polyvinyl alcohol. J Mol Liq 218:191–197
16. Gupta VK, Tyagi I, Agarwal S, Sadegh H, Shahryari-ghoshekandi R, Yari M, Yousefi-nejat O (2015) Experimental study of surfaces of hydrogel polymers HEMA, HEMA-EEMA-MA, and PVA as adsorbent for removal of azo dyes from liquid phase. J Mol Liq 206:129–136
17. Zare K, Sadegh H, Shahryari-ghoshekandi R, Maazinejad B, Ali V, Tyagi I, Agarwal S, Gupta VK (2015) Enhanced removal of toxic congo red dye using multiwalled carbon nanotubes: kinetic, equilibrium studies and its comparison with other adsorbents. J Mol Liq 212:266–271
18. Sadegh H, Mazloumbilandi M, Chahardouri M (2017) Low-cost materials with adsorption performance. In: Martínez L, Kharissova O, Kharisov B (eds) Handbook of ecomaterials. Springer, Cham, pp 1–33
19. Anjaneyulu Y, Sreedhara Chary N, Raj SSD (2005) Decolourization of industrial effluents-available methods and emerging technologies—a review. Rev Environ Sci Biotechnol 4:245–273
20. Aleksic M, Kusic H, Koprivanac N, Leszczynska D, Bozic AL (2010) Heterogeneous Fenton type processes for the degradation of organic dye pollutant in water—the application of zeolite assisted AOPs. Desalination 257:22–29
21. Ilinoiu EC, Pode R, Manea F, Colar LA, Jakab A, Orha C, Ratiu C, Lazau C, Sfarloaga P (2013) Photocatalytic activity of a nitrogen-doped TiO_2 modified zeolite in the degradation of reactive yellow 150 azo dye. J Taiwan Inst Chem Eng 44:270–278
22. Fu J, Kyzas GZ (2014) Wet air oxidation for the decolorization of dye wastewater: an overview of the last two decades. Chin J Catal 35:1–7
23. Bhargava SK, Tardio J, Prasad J, Foger K, Akolekar DB, Grocott SC (2006) Wet oxidation and catalytic wet oxidation. Ind Eng Chem Res 45:1221–1258
24. Levec J, Pintar A (2007) Catalytic wet-air oxidation processes: a review. Catal Today 124:172–184
25. Chan SHS, Wu TY, Juan JC, The CY (2011) Recent developments of metal oxide semiconductors as photocatalysts in advanced oxidation processes (AOPs) for treatment of dye wastewater. J Chem Technol Biotechnol 86:1130–1158
26. Das M, Bhattacharyya KG (2014) Oxidation of Rhodamine B in aqueous medium in ambient conditions with raw and acid-activated MnO_2, NiO, ZnO as catalysts. J Mol Catal Chem 391:121–129
27. Martinez F, Pariente MI, Angel J, Botas JA, Melero JA, Rubalcaba A (2012) Influence of preoxidizing treatments on the preparation of iron-containing activated carbons for catalytic wet peroxide oxidation of phenol. J Chem Technol Biot 87:880–886
28. Bhatnagar A, Hogland W, Marques M, Sillanpaa M (2013) An overview of the modification methods of activated carbon for its water treatment applications. Chem Eng J 219:499–511
29. Dukkanci M, Gunduz G, Yilmaz S, Prihod'ko RV (2010) Heterogeneous Fenton-like degradation of Rhodamine 6G in water using CuFeZSM-5 zeolite catalyst prepared by hydrothermal synthesis. J Hazrad Matter 181:343–350
30. Kondru AK, Kumar P, Chand S (2009) Catalytic wet peroxide oxidation of azo dye (Congo red) using modified Y zeolite as catalyst. J Hazard Mater 166:342–347
31. Ramirez JH, Vicente MA, Madeira LM (2010) Heterogeneous photo-Fenton oxidation with pillared clay-based catalysts for waste water treatment: a review. Appl Catal B Environ 98:10–26
32. Sarma GK, SenGupta S, Bhattacharyya KG (2011) Methylene blue adsorption on natural and modified clays. Sep Sci Technol 46:1602–1614
33. Nezamzadeh-Ejhieh A, Shahriari E (2014) Photocatalytic decolorization of methyl green using Fe(II)-o-phenanthroline as supported onto zeolite Y. J Ind Eng Chem 20:2719–2726
34. Tekbas M, Yatmaz HC, Bektas N (2008) Heterogeneous photo-Fenton oxidation of reactive azo dye solutions using iron exchanged zeolite as a catalyst. Microporous Mesoporous Mater 115:594–602
35. APHA (1989) In: Clesceri LS, Greenberg AE, Trussell RR (eds) Standard methods for the examination of water and wastewater. American Public Health Association, Washington DC, pp 12–13
36. Singh L, Rekha P, Chand S (2016) Cu-impregnated zeolite Y as highly active and stable heterogeneous Fenton like catalyst for degradation of Congo red dye. Sep Purif Technol 170:321–336
37. Hriljac JJ, Eddy MM, Cheetham AK, Donohue JA, Ray GJ (1993) Powder neutron diffraction and 29Si MAS NMR studies of siliceous zeolite Y. J Solid State Chem 106:66–72
38. Chen A, Sun XM (2008) Decolorisation of KN-R catalysed by Fe containing Y and ZSM-5 zeolites. J Hazard Matter 156:568–575
39. Rache ML, Garcia AR, Zea HR, Silva AMT, Madeira LM, Ramirez JH (2014) Azo dye orange II degradation by the heterogeneous Fenton-like process using a zeolite Y-Fe catalyst- Kinetics with a model based on Fermi's equation. Appl Catal B Environ 146:192–200
40. Aravindhan R, Fathima NN, Rao JR, Nair BU (2006) Wet oxidation of acid brown dye by H_2O_2 using heterogeneous catalyst Mn-Salen-Y-Zeolite: a potential catalyst. J Hazard Matter 138:152–159
41. Tayade RJ, Natarajan TS, Bajaj HC (2009) Photocatalytic degradation of methylene blue dye using ultraviolet light emitting diodes. Ind Eng Chem Res 48:10262–10267
42. Bhattacharya KG, SenGupta S, Sarma GK (2015) Kinetics, equilibrium isotherms and thermodynamics of adsorption of Congo red onto natural and acid treated kaolinite and montmorillonite. Desalin Water Treat 53(2):530–542
43. Dutta K, Mukhopadhyay S, Bhattacharjee S, Chaudhury B (2001) Chemical oxidation of methylene blue using a Fenton-like reaction. J Hazard Mater B84:57–71